



Tzemanaki, A., Raabe, D., & Dogramadzi, S. (2011). Development of a novel robotic system for hand rehabilitation. In *24th International Symposium on Computer-Based Medical Systems (CBMS)* Institute of Electrical and Electronics Engineers (IEEE).
<https://doi.org/10.1109/CBMS.2011.5999150>

Peer reviewed version

Link to published version (if available):
[10.1109/CBMS.2011.5999150](https://doi.org/10.1109/CBMS.2011.5999150)

[Link to publication record in Explore Bristol Research](#)
PDF-document

This is the author accepted manuscript (AAM). The final published version (version of record) is available online via IEEE at <https://ieeexplore.ieee.org/document/5999150> . Please refer to any applicable terms of use of the publisher.

University of Bristol - Explore Bristol Research

General rights

This document is made available in accordance with publisher policies. Please cite only the published version using the reference above. Full terms of use are available:
<http://www.bristol.ac.uk/red/research-policy/pure/user-guides/ebr-terms/>

Development of a novel Robotic System for Hand Rehabilitation

Tzemanaki A., Raabe D. and Dogramadzi S.

Bristol Robotics Laboratory, University of the West of England

toniatze@gmail.com; Daniel.Raabe@brl.ac.uk; Sanja.Dogramadzi@uwe.ac.uk

Abstract

Rehabilitation Robotics involves the use of robotic systems as an enabling technology for people with kinetic problems, in order to help them recover from a physical trauma. This paper presents the investigation of a robotic system for stroke and post hand-surgery patient rehabilitation, in order to gradually regain flexibility in their finger-joints by passively extending and flexing their fingers. It includes one linear actuator for each finger and a thin-film force sensor at each fingertip as a safety measure against over-straining the finger-joints. Prior to designing the system, kinematic and dynamic models of a human hand have been derived and simulated in MATLAB. Data obtained from this model show a strong correlation to natural human hand movements, recorded in this study using a 6 DoF motion capture system. Design of the robotic system is performed using UGS NX6 software.

1. Introduction

Hands are the basic tool for physically manipulating the environment. After a stroke, gripping a glass or simply opening the fists is typically too hard to achieve. Impaired hand function is one of the most frequently persisting consequences of a stroke, which may result in the shortening of soft tissue, skin, tendons and muscles.

Stroke is the 2nd most common cause of death^{[1], [2]} and the leading cause of severe adult disability worldwide. For those who survive, the recovery of neurological impairment takes place over a variable time interval. About 30% will fully recover within three weeks, rising to nearly 50% by six months. Besides stroke, hand therapy has a crucial role in the recovery from hand injuries or surgical operations^[3]. Among all disabling work injuries in the United States, almost 17% involve the fingers, while over 25% of athletic injuries involve the hand or the wrist^[4].

Post-operative treatment plays an important role in optimal recovery of the fingers' strength and range of motion. Rehabilitative therapy should begin as soon as a stroke patient is stable, usually within 24 to 48 hours after a stroke^[5]. Likewise, after surgery, depending on the case, the surgeon may prescribe painkilling drugs to manage the patient's discomfort and advise that the physiotherapy should start immediately.

At home, rehabilitation program can be tailored for the patients' needs and follow individual schedules, giving them a chance to practice in the context of their own environment. Nevertheless, the major disadvantage of home-based rehabilitation programs is a lack of specialised equipment. Easy-to-use domestic devices that help patients regain movement in their hands would constitute a huge step towards the direction of home-based rehabilitation. Using them either as a complementary method to the regular treatment or as the primary one would result in a faster recovery.

2. Background

Range of Motion (ROM) activities are basic techniques that focus on motor control for evaluation of the movement as well as for therapy. ROM is the full extent of joint motion. In order to maintain normal ROM, the movement of the joints must cover the available range periodically. ROM activities help maintain joint mobility, minimise loss of tissue flexibility and minimise contracture formation. There are four types: Passive ROM (PROM), Active ROM (AROM), Active-Assistive ROM (A-AROM) and Self-Assistive ROM (S-AROM). AROM is used when the patient is able to contract their muscles actively; if the muscles are too weak A-AROM is preferred until they gain control of their ROM. Active ROM is more beneficial than Passive ROM, as it prevents muscle atrophy since the patient voluntarily controls the muscles, while it also assists circulation to a further extent than PROM does. However, when the patient is not able or not supposed to actively move the specific segment of the body or when there is acute, inflamed

tissue and hence active motion would be detrimental to the healing process, PROM is more beneficial.

Continuous Passive Motion (CPM) was introduced by Salter^[6] and refers to passive motion performed by a mechanical device that moves a joint continuously through a controlled ROM. Salter demonstrated that continual passive motion has beneficial healing effects on diseased or injured joint structures and soft tissues [6]. Kisner and Colby conclude, regarding Salter's research, that CPM leads to earlier discharge from hospital [7].

An incident of a stroke will be followed by a period of cerebral shock, which can vary in time from a few days to few months and may progress in different stages. Persistence of hypotonicity (flaccid stage) is the most disabling stage, during which the person's arm is floppy and cannot be supported in space because of muscle weakness and low tone. The next stage is when movements start again in the limbs (recovery stage).

Identifying the significance of the problem and thus encouraging research on the subject has led to the formation of several different approaches in building a hand-rehabilitation system.

Before actuated systems became popular, splinting was and perhaps still is the most common and well accepted treatment modality in hand rehabilitation. The very presence, however, of a splint is inhibiting the free movement and use of the hand^[8]. SaebFlex^[9] belongs in the category of dynamic splints and is a purely mechanical device, that positions the wrist and fingers in preparation for grasp and release activities.

Sensory-monitoring systems such as [10], aim to sense the movement of the hand and simulate it in a graphical environment of a computer, motivating patients to perform tasks and then marking them on how 'well' they completed them. This system consists of a series of sensors providing feedback in order to control the resistance in hand exercises. Another example of virtual rehabilitation is presented in [11], combining virtual reality with traditional therapy techniques, while it is based on the commercially available Microsoft Xbox video game and Essential Reality P5 gaming glove.

Passive range of motion devices help or gently force the patient's fingers to move. Such a system is 'Amadeo'^[12], in which emphasis is given mostly to the fingertip and joints are moved indirectly, while [13] combines robotics and interactive gaming to facilitate repetitive performance of task specific exercises. The rehabilitation system presented in [14] uses interactive control to assist the patient undergo rehabilitation exercises, in three modes of assistance: passive, "assisting as needed" and active. In [15] an exoskeleton is designed to facilitate movement, especially of pinch movement, intended to provide

independent control of all three joints of the index. The system in [16] consists of two components; the finger joints of the left hand are attached to an exoskeleton, being controlled by the finger joints of the right hand wearing a data glove.

3. Mathematical model of a human hand

In order to understand the finger movements of a healthy hand, a kinematic model, characterized by ideal joints and simple segments, has been developed. The joints of the finger are illustrated in figure 1.

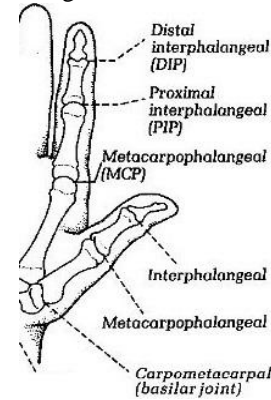


Figure 1. Bones and joints of the hand (adapted: American Society for Surgery of the Hand)

The PIP and DIP joints of the fingers are hinge joints capable of only flexion and extension, while the MCP are saddle joints and hence, capable of abduction and adduction motions as well. In [17] and [18] it is proposed that the CMC joint of the thumb is a 2 DoF one; however, in [19] it is considered to have axial rotation as well. Furthermore, [20] suggests that each of the fingers is defined by 5 DoF and 4 links, while the thumb by 4 DoF and 3 links. Various models are used; [21] represents the hand by a rigid linkage system incorporating 22+3 DoF (3 added DoFs for the wrist). They consider the MCP joint of the thumb as a 2 DoF and the CMC as a 3 DoF one. In [22] fingers are also considered to have 4 DoFs and the thumb 3 DoFs, while 3 DoFs are added for the wrist.

The approach adopted in this paper considers the thumb to have 5 DoFs in total and each of the fingers 4 DoFs. The 21 DoFs model is sufficient for all functional moves and is preferred for its lower degree of complexity. Using the Denavit-Hartenberg notation and given the joint angles, the fingertip position in the palm frame is calculated by the kinematic model. The angles that describe the rotations of the joints are θ_1 , θ_2 for the MCP, θ_3 for the PIP and θ_4 for the DIP of the index/middle/ring/little finger, while for the thumb they are θ_1 , θ_2 , θ_3 for the CMP, θ_4 for the MCP and θ_5 for the IP.

Table 1. Denavit-Hartenberg parameters

Index/Middle/Ring/Little					Thumb				
Link	a_i	α_i	d_i	θ_i	Link	a_i	α_i	d_i	θ_i
1	0	-90	0	θ_1	1	0	-90	0	θ_1
2	ℓ_1	0	0	θ_2	2	0	-90	0	θ_2
3	ℓ_2	0	0	θ_3	3	ℓ_1	0	0	θ_3
4	ℓ_3	0	0	θ_4	4	ℓ_2	0	0	θ_4
					5	ℓ_3	0	0	θ_5

Figure 2 demonstrates the graphical model of the index (left) and the thumb (right).

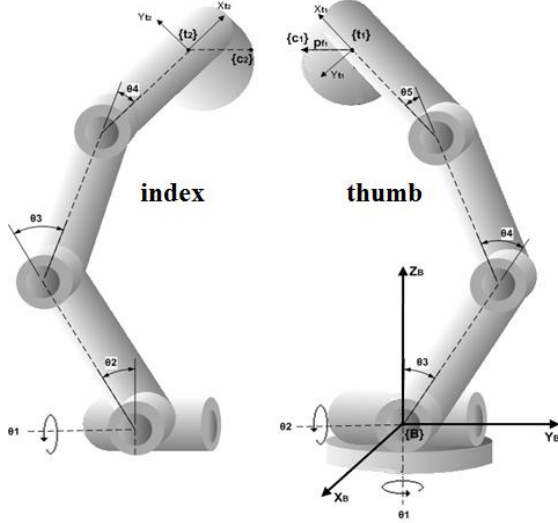


Figure 2. Graphical model of thumb and index

If $c_{ij} = \cos(\theta_i + \theta_j)$ and $s_{ij} = \sin(\theta_i + \theta_j)$, the Homogenous Transformations that relate frame $\{t\}$ to the inertial frame at the base of each finger are:

$$g_{t1} = \begin{bmatrix} c_1 c_2 c_{345} + s_1 s_{345} & -c_1 c_2 s_{345} + s_1 c_{345} & -c_1 s_2 & c_1 c_2 h_{10} + s_1 h_{11} \\ s_1 c_2 c_{345} - c_1 s_{345} & -s_1 c_2 s_{345} - c_1 c_{345} & -s_1 s_2 & s_1 c_2 h_{10} - c_1 h_{11} \\ -s_2 c_{345} & -s_2 s_{345} & -c_2 & -s_2 h_{10} \\ 0 & 0 & 0 & 1 \end{bmatrix}$$

$$g_{t2} = \begin{bmatrix} c_1 c_{234} & -c_1 c_2 s_{345} + s_1 c_{345} & -c_1 & c_1 h_{20} \\ s_1 c_{234} & -s_1 c_2 s_{345} - c_1 c_{345} & -s_1 & s_1 h_{20} \\ -s_{234} & -c_{234} & 0 & -h_{21} \\ 0 & 0 & 0 & 1 \end{bmatrix}$$

where: $h_{10} = \ell_1 c_3 + \ell_2 c_{34} + \ell_3 c_{345}$, $h_{11} = \ell_1 s_3 + \ell_2 s_{34} + \ell_3 s_{345}$, $h_{20} = \ell_1 c_2 + \ell_2 c_{23} + \ell_3 c_{234}$ and $h_{21} = \ell_1 s_2 + \ell_2 s_{23} + \ell_3 s_{234}$.

The Lagrange equation for the system of a finger moving unrestricted in space is the following:

$$M(\theta)\ddot{\theta} + C(\theta, \dot{\theta})\dot{\theta} + G(\theta) = \mathbf{u}$$

where $\theta \in \mathbf{R}^{5 \times 1}$ or $\mathbf{R}^{4 \times 1}$ is the joint angles vector (5 DoF or 4 DoF correspondingly), $M(\theta) \in \mathbf{R}^{5 \times 5}$ or $\mathbf{R}^{4 \times 4}$ is the mass matrix of the finger, $C(\theta, \dot{\theta}) \in \mathbf{R}^{5 \times 1}$ or $\mathbf{R}^{4 \times 1}$ are the centrifugal and Coriolis forces, $G(\theta) \in \mathbf{R}^{5 \times 1}$ or $\mathbf{R}^{4 \times 1}$ is the gravity forces vector and $\mathbf{u} \in \mathbf{R}^{5 \times 1}$ or $\mathbf{R}^{4 \times 1}$ is torque vector in the joints. The control of the joints could be joint-space control or Cartesian-space control; joint-space control, however, seems more suitable as it focuses on the joint mobilisation and not the fingertip's actual

position. Figure 3 shows the initial and final position of the fingers, respectively.

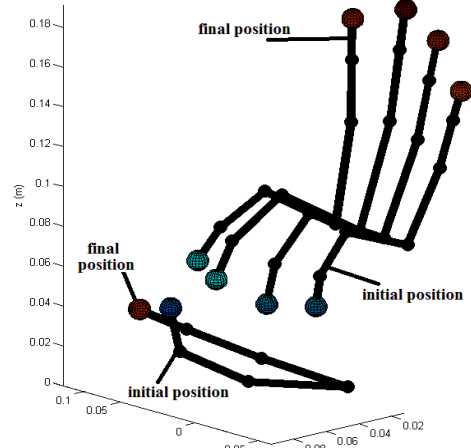


Figure 3. Initial and final position

4. Fingers' trajectories exploration

Figure 4 demonstrates the trajectory that the fingertip follows during joint-space control simulation. Generally, the trajectory depends on the nature of the task. However, when trying to recover from kinetic disability conditions, the goal, as explained previously, is to mobilise the joints of the patient's hand and not to move the fingers in the most effective way to a desired position. Nevertheless, there is a limit on how much we can rely on simulated results; we need to validate the fact that the trajectories in figure 4 are natural trajectories of human fingers during extension or flexion.

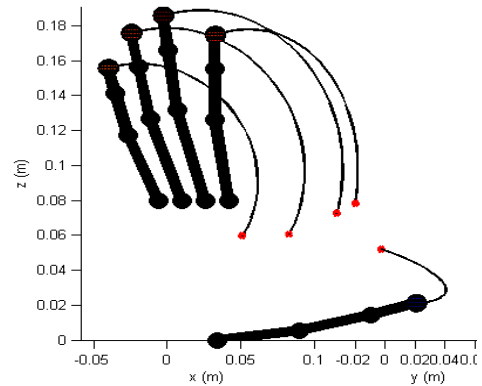


Figure 4. Tip trajectory (red is the initial position)

Motion capture devices track the position of reflective markers in 3D space, using infra-red cameras that provide opto-electric data. The experiment involved placing a marker at each end of a person's finger-links (see Fig. 5); the person flexes and extends the finger slowly moving every joint in a natural fashion. Three more markers were placed on the palm,

to derive smooth data and eliminate any potential noise caused by the hand shaking. Markers were placed only on the middle finger, assuming that other fingers' motion is similar.



Figure 5. Location of the markers on the experiment glove

Figure 6a delineates the trajectories that were produced; each curve represents a point attached to a finger-joint. Comparing the trajectories obtained from VICON and MATLAB (figure 6b), we observe that they are similar and, hence, the results of the simulation are valid.

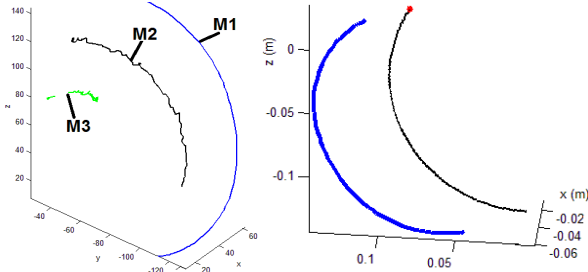


Figure 6. a) Trajectories as captured by VICON
b) comparison between MATLAB (black) and VICON (blue)

5. Concept design of the prototype

The aim of this rehabilitation system is to meet the needs of patients with weak muscles, e.g. stroke patients in the flaccid stage. It takes into consideration movement in all joints separately, while each finger is independent from the others. The mechanism, shown in Figure 7, utilizes linear actuators, one for each finger (for demonstration purposes, only two actuators appear). Each actuator has a universal joint attached to its base, and a revolute joint attached to its end; both are passive and contribute to producing a movement that follows the natural trajectory of the finger. The hand rest has slider parts on which the part of the finger that is not exercised rests. This is achieved by a set of small magnets that are fixed on these parts, while opposing magnets are sewn inside a glove that the patient wears. This way, it is possible to fix the first link and exercise the PIP and DIP (in that case PIP is mobilised more) or fix the first and the second link and exercise only the DIP joint.

The advantage of this system is most of all its flexibility. The actuators can move across the y axis,

indicated in figure 7, while the hand-rest can move forth and back in x direction. The slider parts can also be fixed in any position that is convenient for the fingers. The structure is very simple, while the addition of a revolute and a universal joint to each actuator provides an extra degree of freedom to the finger, as it can move not only parallel to plane xz but also to yz (when the first link is not fixed to the slider part).

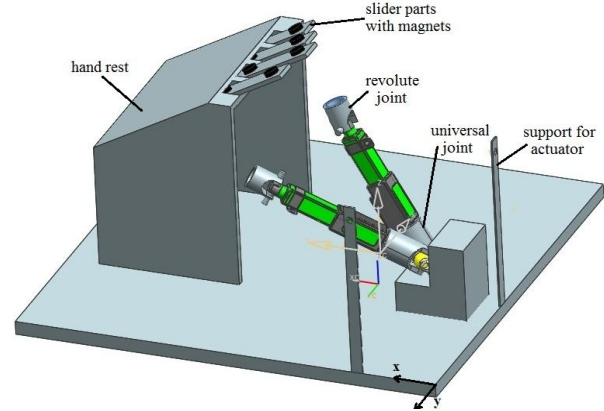


Figure 7. Concept drawing

6. CAD and multi-body simulation

Siemens software package NX supports dynamic multi-body simulations. In this study, what is of interest is the trajectory of the finger passively moved by the actuator. For this reason, a hand with joints and links as described in section 3 was modelled in the same software. Figures 8 a and b show the movement of the last link of the index, while the trace of the fingertip is also indicated. It is obvious that the trajectory is a curve that resembles the natural motion of the finger as it was examined in MATLAB and VICON.

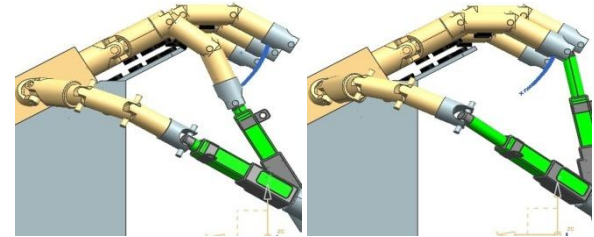


Figure 8. a) Index in initial position b) Final position

7. Manufacturing and commissioning of the prototype

The physical structure, displayed in figure 9, was built on a FDM Titan rapid prototyping machine. Instead of a universal joint at the base of each actuator, a ball joint was created, being less delicate and easier to construct.

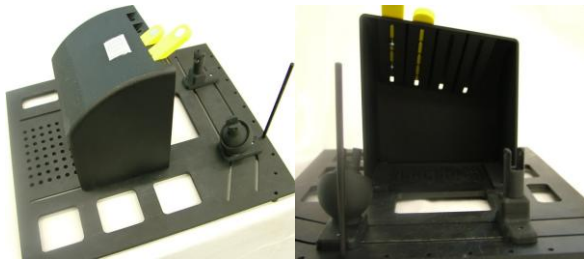


Figure 9. Physical structure made by the RP machine

In order to find the most efficient, cheap and suitable solution, a variety of actuators has been considered. The most compact (and at the same time cheap) solution is the Firgelli L12 actuator with 30 or 50 mm of stroke; both of them will provide adequate stroke length, while their body dimensions are not too big. In this project, a stroke of 30 mm was chosen, as a start, to experiment with the operation and size of the structure.

The L12-P actuator is designed to push or pull loads along its full stroke length and can provide an analogue position feedback signal that can be inputted into an external controller. The Linear Actuator Control (LAC) board is a stand-alone closed-loop control board that has the possibility to manually adjust the sensitivity of the actuator control algorithm, the speed of the actuator and set the minimum and maximum acceptable positions of the actuator stroke. The board, during the evaluation phase, was operated in two modes:

USB Mode: the actuator was controlled using a computer and the Firgelli LAC Configuration Utility, where the user can also make advanced settings that allow fine control over the controller response.

PWM Mode: the control is done using a single digital output pin from an external micro controller (in this case Arduino Uno). The desired position is encoded as the duty cycle of a 3.3 Volt, 1 kHz square wave. The percentage of the duty cycle sets the actuator position to the same percentage of the full stroke extension.

In addition to the actuator, a Flexiforce A201 (Tekscan) sensor was used that measured forces in the . in the range of 0-20 lb. This sensor is a paper-thin and flexible printed circuit, with a sensing area at its end. The sensor acts as a variable resistor in an electrical circuit; when unloaded, its resistance is greater than $5M\Omega$, while when a force is applied the resistance decreases. In order to integrate it into the application, the sensor is incorporated into a force-to-voltage circuit, which uses an inverting operational amplifier arrangement to produce an analogue output based on the sensor resistance and a fixed resistance (R_F). The sensor was calibrated using a structure that consisted of a set of scales and a pivot structure, on which the

weights were placed, while a multimeter was used to measure the output voltage or resistance of the sensor. The produced by the calibration experiment load-voltage curve is displayed in figure 10. Known force (calibration weights) was applied on the sensing area of the sensor and the output voltage was measured. The curves of the graph describe a different experiment; red is direct contact with the sensing area, blue is soft surface and black is aluminium distribution surface. Each curve is the result of the average of three repetitions of each experiment. In this case the circuit is driven by $V_T = -5V$ excitation voltage and the reference resistance is fixed at $R_f = 47k\Omega$. The output voltage is theoretically calculated using the formula $V_{out} = -V_T \left(\frac{R_f}{R_S} \right)$ (R_S is the sensor's resistance).

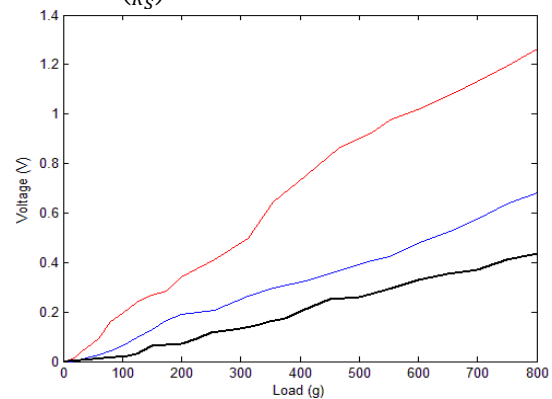


Figure 10. Load-Voltage curve

As shown in Figure 10, the sensor's response follows a pattern, which is approximately linear. However the magnitude of the voltage changes depending on the type of contact. It has also been noted that during the first two experiments (red and blue) the measurement was difficult to take; a slight offset from the initial contact point would dramatically change the response. The aluminium surface distributes the force almost evenly across the sensing area and therefore, is considered as the most reliable calibration method.

There are 22 magnets needed for the system. 13 magnets are sewn into a glove (one for each link of the fingers and 1 for the thumb's fingertip – see fig. 11). 4 are fixed on the slider parts of the rest that hold the fingers and 1 for each actuator, 5 in total, fixed inside the revolute joint part that covers each fingertip.



Figure 11. Location (red dots) of the magnets in the glove

Figure 12 shows the connections between all the electronic components. According to the characteristics of the components, the power source needed for the application is 6.5V and -5V for the sensor, 5-24 V for the LAC board and 6-12V for the Arduino. Therefore, common adaptors from 230 Vac to 6.5 Vdc and from 230 Vac to -5 Vdc (they could also be integrated into one) can be used to power the system, without having to use batteries which will have to be recharged or changed frequently.

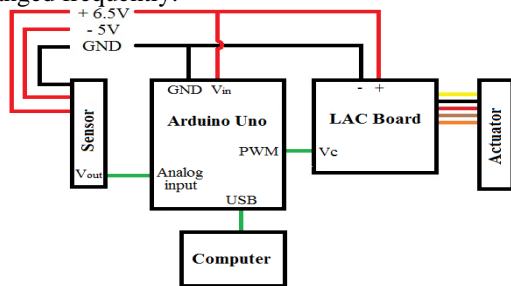


Figure 12. Connections of the electronic components

8. Conclusions and future work

A model of a human hand and the fingers' trajectories were analysed in order to build the presented rehabilitation system, based on CPM and designed for patients in their first stage of recovery. It is low-cost, portable and can be adjusted to most hand sizes.

Later enhancements could include actuators of a bigger stroke for some of the fingers, while an interactive screen could help the patients choose their program and level of difficulty. Vibration motors can also be added, in order to relax and prepare the hand for the exercises. The adjustability of the system can increase by making the hand rest move in the vertical direction as well.

10. References

[1] World Health Organisation, *Factsheets*, 2004, [online] Available at: www.who.int/mediacentre/factsheets/fs310.
 [2] Amer. Heart Assoc., *Int. Disease Statistics*, 2007, [online] Available at: www.americanheart.org/downloadable/heart/1177593979236FS06INTL07.pdf.
 [3] BSSH, *What is Hand Therapy*, 15 June 2010 [online]. Available at: www.bssh.ac.uk/patients/whatishandtherapy.
 [4] Surgery.com, *Hand injuries demographics*, [online] Available at: www.surgery.com/procedure/hand-surgery/demographics.
 [5] Nat. Inst. of Neurological Disorders and Stroke. *Post-Stroke Rehabilitation Fact Sheet*. [online] Available at: www.ninds.nih.gov/disorders/stroke/poststroke rehab.htm.
 [6] RB. Salter, et al, "The biological effects of continuous passive motion on the healing of full thickness defects in

articular cartilage. An experimental investigation in the rabbit", *J. of Bone and Joint Surgery*, Raven Press, New York, 1980, 62:1232-1251.

[7] C. Kisner and LA. Colby, *Therapeutic Exercise, foundations and techniques*. Davis Company, United States of America, 2007.

[8] Brand, W. P. The forces of dynamic splinting: ten questions before applying a dynamic splint to the hand. In: Hunter, Schneider, Mackin and Callahan, eds. 1990. *Rehabilitation of the hand: surgery and therapy*. The C. V. Mosby Company, United States of America, Ch. 87.

[9] Saebo, *Saeboflex*, 2002, [online] Available at: www.saebo.com/products/saeboflex.

[10] News@Northeastern, *Helping Hands*, [online] Available at: www.northeastern.edu/news/stories/2009/12/capstoneglov e.html.

[11] K. Morrow, et al, "Low-cost Virtual Rehabilitation of the Hand for Patients Post-Stroke", *2006 Int. Workshop on Virtual Rehabilitation*, pp.6-10.

[12] Tyromotion company, *Amadeo*, 2008, [online] Available at: www.tyromotion.com/index.php?id=13&L=1.

[13] Northeastern University Robotics and Mechatronics Laboratory. 2009. *2 DoF Robotic Hand Rehabilitation System With Interactive Gaming*. [online] Available at: www.robots.neu.edu/research.htm.

[14] Y.Y. Huang, K.H. Low, "A multi-disciplinary approach for effective hand rehabilitation with clinical-based assessment outcomes", *CASE 2009. IEEE Int. Conf. on Automation Sci. and Eng.*, 2009, p. 597 - 603, 22-25 Aug. 2009.

[15] T.T. Worsnopp, et al, "An Actuated Finger Exoskeleton for Hand Rehabilitation Following Stroke". *2007 IEEE 10th Intern. Conf. Proc. on Rehabilitation Robotics*, Noordwijk, The Netherlands, June 12-15, p. 896.

[16] Yamaura, H., Matsushita, K., Kato, R., Yokoi, H. "Develop. of Hand Rehabilitation System for Paralysis Patient – Universal Design Using Wire-Driven Mechanism", *31st Annu. Int. Conf. of the IEEE EMBS*, Minneapolis, Minnesota, USA, September 2-6, 2009.

[17] T. Blakely Y. Matsuoka, "Software framework for human neuromuscular behaviour", *2009 ICRA '09. IEEE Int. Conf. on Robotics and Automation*, p.4069 - 4073, 12-17 May 2009.

[18] Cerveri, P. et al, "Finger kinematic modelling and real-time hand motion estimation", *Ann. of Biomedical Eng.*, 2007, Vol. 35, No. 11, pp. 1989-2002.

[19] B.O. Buchholz, and T.J. Armstrong, "A kinematic model of the human hand to evaluate its prehensile capabilities". *J. of Biomechanics*, 1992, Vol. 25, No. 2, pp. 149-162.

[20] S. Cobos, et al, "Efficient Human Hand Kinematics for Manipulation Tasks", *IEEE/RSJ Inter. Conf. on Intelligent Robots and Syst.*, Acropolis Conv. Center, Nice, France, Sept, 22-26, 2008, pp. 2246-2251.

[21] X. Yang, J. Park, K. Jung, H. You, "Develop. and Evaluation of a 25-Degree of Freedom Hand Kinematic Model", *Proc. of the 2008 Fall Conf. of the Ergonomics Society of Korea*.

[22] Dragulescu, D. et al, "3D active workspace of human hand anatomical model", *BioMedical Eng. OnLine* 2007, 6:15, doi: 10.1186/1475-925X-6-15.